

Probabilistic Safeguard for Reinforcement Learning Using Safety Index Guided Gaussian Process Models

Weiye Zhao*, Tairan He*, Changliu Liu

Robotics Institute, Carnegie Mellon University, Pittsburgh, PA 15213 USA
weiyezha@andrew.cmu.edu, tairanh@andrew.cmu.edu, cliu6@andrew.cmu.edu

Abstract

Safety is one of the biggest concerns to applying reinforcement learning (RL) to the physical world. In its core part, it is challenging to ensure RL agents persistently satisfy a hard state constraint without white-box or black-box dynamics models. This paper presents an integrated model learning and safe control framework to safeguard any agent, where its dynamics are learned as Gaussian processes. The proposed theory provides (i) a novel method to construct an offline dataset for model learning that best achieves safety requirements; (ii) a parameterization rule for safety index to ensure the existence of safe control; (iii) a safety guarantee in terms of probabilistic forward invariance when the model is learned using the aforementioned dataset. Simulation results show that our framework guarantees almost zero safety violation on various continuous control tasks.

1 Introduction

While reinforcement learning (RL) has achieved impressive results in games like Atari (Mnih et al. 2013), Go (Silver et al. 2017) and Starcraft (Vinyals et al. 2019), the lack of safety guarantee limits the application of RL algorithms to real-world physical systems such as robotics (Berkenkamp et al. 2017). In its core part, it is critical to ensure that RL agents persistently satisfy a hard state constraint defined by a *safe set* (e.g., a set of non-colliding states) in many robotic applications (Zhao, He, and Liu 2021). Though many works design constrained RL algorithms (Uchibe and Doya 2007; Achiam et al. 2017; Wachi et al. 2018; Yang et al. 2021), the trial-and-error mechanism of these methods makes it hard to avoid safety violations during policy learning.

On the other hand, when the dynamics model of the system is accessible, energy-function-based safe control methods can achieve the safety guarantee, i.e., persistently satisfying the hard state constraint. These methods (Khatib 1986; Ames, Grizzle, and Tabuada 2014; Liu and Tomizuka 2014; Gracia, Garelli, and Sala 2013; Zhao, He, and Liu 2021) first synthesize an energy function such that the safe states have low energy, and then design a control law to satisfy the safe action constraints, i.e., to dissipate energy. Then these methods ensure *forward invariance* inside the safe set (i.e., the system state will never leave the safe set). However, the major

limitation of these methods is that they exploit either white-box dynamics models (e.g., analytic form) (Khatib 1986; Ames, Grizzle, and Tabuada 2014; Liu and Tomizuka 2014; Gracia, Garelli, and Sala 2013) or black-box dynamics models (e.g., digital twin simulators) (Zhao, He, and Liu 2021), while these models are not easily accessible in complex environments. Practically, compared to dynamics models (i.e., a full mapping from the current state and control to the next state), it is easier to obtain samples of the dynamic transitions in real-world applications (Huang et al. 2018; Caesar et al. 2020). This paper investigates approaches to utilize these transition samples to achieve safety guarantees under the energy-function-based safe control framework, while relaxing the requirements of white-box or black-box dynamics models. In our methods, we leverage Gaussian Process (GP) to learn a statistical dynamics model due to (i) GP’s reliable estimate of uncertainty (Williams and Rasmussen 2006); (ii) its well-established theory on uniform error bounds (Srinivas et al. 2009, 2012; Chowdhury and Gopalan 2017; Kanagawa et al. 2018; Lederer, Umlauf, and Hirche 2019). Instead of online learning where safety and efficiency can be compromised as the distribution of data used in learning cannot be fully anticipated, our dynamics model is learned based on an offline constructed dataset. The offline constructed dataset offers good control over the data distribution, which could further lead to (i) reliable convergence in model learning; and (ii) good safety guarantees.

The main contribution of this paper is a theory to probabilistically safeguard robot policy learning using energy-function-based safe control with a GP dynamics model learned on an offline dataset. The overall pipeline of our method is shown in Figure 1. To achieve our goal of safeguarding RL agents with GP dynamics model, we first show how to construct the dataset for model learning and how to design the associated energy function (called *safety index*) so that there always exists a feasible safe control for any state. Secondly, we show how to design a safeguard for arbitrary RL agents to guarantee forward invariance during policy learning. The method is evaluated on various challenging continuous control problems where the RL agents achieve almost zero constraint violation during policy learning.

*These authors contributed equally.

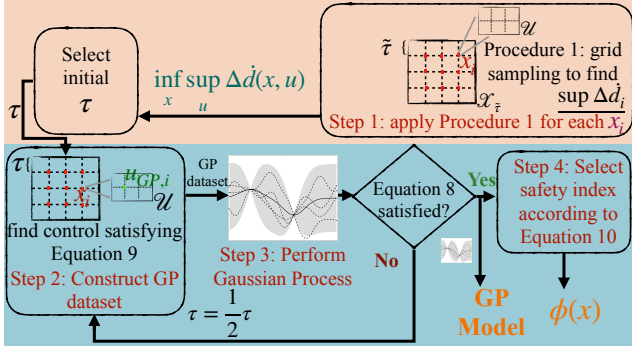


Figure 1: The flow chart for UAISSA *Offline Stage*: (i) select proper discretization gap based on system properties (orange background); (ii) construct the offline dataset for GP and design parameters of the safety index (blue background).

2 Related Work

The desire to make learning agents persistently satisfy a state constraint drives many safe learning works to study state-wise safety which can be divided into three categories.

1. The first category of works assumes the knowledge of white-box or black-box dynamics models, and achieve safe exploration by safeguarding nominal controls from RL (Ferlez et al. 2020; Fisac et al. 2018; Cheng et al. 2019; Zhao, He, and Liu 2021). Specifically, ShieldNN (Ferlez et al. 2020) designs a safety filter neural network with safety guarantees. However, ShieldNN is specially designed for an environment with the kinematic bicycle model (KBM) (Kong et al. 2015) as the dynamics model, which is hard to generalize to other problem scopes. Implicit safe set algorithm (ISSA) (Zhao, He, and Liu 2021) achieves zero violation during RL training but requires a black-box dynamics model for one-step simulations.
2. The second category of works achieves safety using online learned models. A safe learning framework based on Hamilton-Jacobi reachability methods is proposed to safeguard policy learning (Li et al. 2020) with online learned GP dynamics models. However, since online learning has no guarantee over the data distribution, the policy may become very conservative in exchange for safety guarantees. Another model-based safe RL framework (Berkenkamp et al. 2017) is proposed to safely explore the environment with online learned dynamics models. Nevertheless, the framework requires a proper Lyapunov function that can be dissipated at all states and an initial safe policy, which are both challenging to get in complex environments.
3. The last category of methods provides safety guarantees based on learned models from offline datasets. (Dean et al. 2019) studies how to construct a dataset, and how to learn the dynamics such that constrained linear quadratic regulator system can be stabilized. However, only linear systems are studied, which limits the applicability to complex nonlinear systems. Some other methods propose to safeguard RL agents based on learned dynamics using neural networks (Dalal et al. 2018) or Gaussian process (Cheng et al. 2019). However, due to the lack of

quantification of uniform error bounds of statistical models, such methods (Dalal et al. 2018; Cheng et al. 2019) can not guarantee safety in theory since the prediction of dynamics may be arbitrarily wrong. Our work can be classified into the third category. To the best of our knowledge, our paper is the first to provide a provable safety guarantee for nonlinear systems based on offline datasets.

3 Problem Background

3.1 Notations

Dynamics Denote $x_t \in \mathcal{X} \subset \mathbb{R}^{n_x}$ as the robot state at time step t ; $u_t \in \mathcal{U} \subset \mathbb{R}^{n_u}$ as the control input to the robot at time step t . And denote $\mathcal{W} := \mathcal{X} \times \mathcal{U}$, which is assumed to be compact. The system dynamics are defined as:

$$x_{t+1} = f(x_t, u_t), \quad (1)$$

where $f : \mathcal{W} \rightarrow \mathcal{X}$ is a function that maps the current robot state and control to the robot state in the next time step. For simplicity, this paper considers deterministic dynamics.

Safety Specification The safety specification requires that the system state should be constrained in a closed subset in the state space, called the safe set \mathcal{X}_S . The safe set can be represented by the zero-sublevel set of a continuous and piecewise smooth function $\phi_0 : \mathbb{R}^{n_x} \rightarrow \mathbb{R}$, i.e., $\mathcal{X}_S = \{x \mid \phi_0(x) \leq 0\}$. \mathcal{X}_S and ϕ_0 are directly specified by users.

3.2 Preliminary

Gaussian Process A Gaussian process (GP) (Williams and Rasmussen 2006) is a nonparametric regression method specified by its mean $\mu_g(z) = \mathbb{E}[g(z)]$ and covariance (kernel) functions $k(z, z') = \mathbb{E}[(g(z) - \mu_g(z))(g(z') - \mu_g(z'))]$. Given N finite measurements $y_N = [y(z_1), y(z_2), \dots, y(z_N)]^T$ of the unknown function $g : \mathbb{R}^D \rightarrow \mathbb{R}$ subject to independent Gaussian noise $v \sim \mathcal{N}(0, \sigma_{\text{noise}}^2)$, the posterior mean $\mu(z_*)$ and variance $\sigma^2(z_*)$ are calculated as:

$$\mu(z_*) = k_*^T(z_*)(K + \sigma_{\text{noise}}^2 I_N)^{-1} y_N \quad (2)$$

$$\sigma^2(z_*) = k(z_*, z_*) - k_*^T(z_*)(K + \sigma_{\text{noise}}^2 I_N)^{-1} k_*(z_*), \quad (3)$$

where $K_{i,j} = k(z_i, z_j)$ and $k_*(z_*) = [k(z_1, z_*), k(z_2, z_*), \dots, k(z_N, z_*)]^T$. In the following discussions, we assume observation is noise-free, i.e. $\sigma_{\text{noise}} = 0$. For most commonly used kernel functions, GP can approximate any continuous function on any compact subset of \mathcal{Z} (Srinivas et al. 2012). In this paper, the dynamics are modeled using GP with the following definition.

Definition 1 (GP Dynamics Model). *The dynamics model of f in (1) is represented as a zero mean Gaussian process with a continuous covariance kernel $k(\cdot, \cdot)$ with Lipschitz constant L_k on the compact set \mathcal{W} .*

Safety Index To ensure system safety, all visited states should be inside \mathcal{X}_S . However, \mathcal{X}_S may contain states that will inevitably go to the unsafe set no matter the control input. Hence, we need to assign high energy values to those inevitably unsafe states, and ensure **forward invariance** in

a subset of the safe set \mathcal{X}_S . Safe Set Algorithm (SSA) (Liu and Tomizuka 2014) synthesizes the energy function as a continuous, piece-wise smooth scalar function $\phi : \mathbb{R}^{n_x} \rightarrow \mathbb{R}$, named, safety index. And we denote its 0-sublevel set as $\mathcal{X}_S^D := \{x | \phi(x) \leq 0\}$. The general form of the safety index was proposed as $\phi = \phi_0^* + k_1 \dot{\phi}_0 + \dots + k_n \phi_0^{(n)}$ where (i) the roots of $1 + k_1 s + \dots + k_n s^n = 0$ are all negative real (to ensure zero-overshooting of the original safety constraints); (ii) the relative degree from $\phi_0^{(n)}$ to u is one (to avoid singularity); and (iii) ϕ_0^* defines the same zero sublevel set as ϕ_0 (to nonlinear shape the gradient of ϕ at the boundary of the safe set). It is shown in (Liu and Tomizuka 2014) that choosing a control that decreases ϕ whenever ϕ is greater than or equal to 0 can ensure forward invariance inside $\mathcal{X}_S \cap \mathcal{X}_S^D$.

3.3 Problem Formulation

The core problem of this paper is to safeguard a nominal controller (i.e., an RL agent) such that all visited states are inside \mathcal{X}_S . In this paper, we are specifically interested in *degree two systems* (i.e., the relative degree from ϕ_0 to u is one), and the safety specification is defined as $\phi_0 = d_{min} - d$ where d denotes the safety status of the system, and the system becomes more unsafe when d decreases. For example, for collision avoidance, d can be designed as the relative distance between the robot and obstacles, which needs to be greater than some threshold d_{min} . Following the rules in (Liu and Tomizuka 2014), we parameterize the safety index as $\phi = \sigma + d_{min}^n - d^n - k\dot{d}$, and $\sigma, n, k > 0$ are tunable parameters of the safety index. It is easy to verify that this design satisfies the three requirements discussed above.

The nominal control is an RL controller which aims to maximize cumulative discounted rewards in an infinite-horizon deterministic Markov decision process (MDP). An MDP is specified by a tuple $(\mathcal{X}, \mathcal{U}, \gamma, r, f)$, where $r : \mathcal{X} \times \mathcal{U} \rightarrow \mathbb{R}$ is the reward function, $0 \leq \gamma < 1$ is the discount factor, and f is the deterministic system dynamics defined in (1), and we can access data samples of f . We then define the discrete-time set of safe control as $\mathcal{U}_S^D(x) := \{u \in \mathcal{U} | \phi(f(x, u)) \leq \max\{\phi(x) - \eta, 0\}\}$. Hence, safeguarding the nominal controller is essentially projecting the nominal control u_t^r to $\mathcal{U}_S^D(x)$ by solving the following optimization:

$$\begin{aligned} \min_{u_t \in \mathcal{U}} & \|u_t - u_t^r\|^2 \\ \text{s.t. } & \phi(f(x_t, u_t)) \leq \max\{\phi(x_t) - \eta, 0\}. \end{aligned} \quad (4)$$

There are several challenges towards solving (4): (i) Firstly, it remains unclear how to verify whether there is a solution of (4) without the knowledge of dynamics f ; (ii) Secondly, it remains unknown how to construct a statistical model of dynamics f that will result in a safety guarantee; (iii) Thirdly, it is challenging to parameterize ϕ such that there is always a feasible solution for (4) at all states; (iv) Lastly, an efficient algorithm for solving (4) during online policy learning remains to be discovered.

Generally, it is nearly impossible to provide a safety guarantee based on statistical models without further assumptions (Berkenkamp et al. 2017). We first introduce an assumption regarding Lipschitz continuity (Vidyasagar 2002).

Assumption 1 (Lipschitz Continuity). *The dynamics $f(\cdot)$ in (1) is L_f Lipschitz continuous with respect to the 1-norm.*

To enable a provable probabilistic safety guarantee, we also assume a reliable statistical model.

Assumption 2 (Well-Calibrated Model). *There exists a GP model (Definition 1) of the dynamics in (1) with posterior mean $(\mu_f(\cdot))$ and covariance matrix $(\Sigma_f(\cdot))$ functions. With $\sigma_f(x, u) = \text{Tr}(\Sigma_f^{\frac{1}{2}}(x, u))$, there exists $\beta_f > 0$ such that with probability at least $(1 - \delta)$ it holds for all $x \in \mathcal{X}$, and $u \in \mathcal{U}$ that $\|f(x, u) - \mu_f(x, u)\|_1 \leq \beta_f \sigma_f(x, u)$.*

This assumption ensures that the confidence intervals of GP prediction cover the true dynamics function with high probability given an appropriate constant β_f . There are well-established theories on uniform error bounds (Srinivas et al. 2009, 2012; Chowdhury and Gopalan 2017; Kanagawa et al. 2018; Lederer, Umlauf, and Hirche 2019) for GP to fulfill Assumption 2.

4 Theory

In this section, we introduce the uncertainty-aware safe set algorithm to tackle the aforementioned challenges. We start by discussing a theory that verifies the feasibility of (4) for all possible states (which is uncountably many) by verifying the feasibility of a similar problem for finitely many states (Proposition 1). Then, we discuss the criteria of dataset construction for model learning and the associated safety index design rule which ensure nonempty set of safe control for all possible system states (Theorem 2). Lastly, we introduce the uncertainty-aware implicit safe set algorithm which generates the safe control efficiently by querying the learned dynamics (Algorithm 1). Under our safe control framework, we show that the system is guaranteed to stay within the safe set (i.e., forward invariance) with high probability (Theorem 4).

4.1 Offline Optimization for Safety Index Synthesis

To ensure there exists a solution to (4) for all states, the parameters of safety index $\phi(\cdot)$ must satisfy:

$$\forall x \in \mathcal{X}, \exists u, \text{ s.t. } \phi(f(x, u)) < \max\{\phi(x) - \eta, 0\} \quad (5)$$

Based on Assumption 1 and Assumption 2, we can make a one-step prediction of the safety index $\phi(f(x, u))$ based on the prediction of dynamics $f(x, u)$. Therefore, we can derive a probabilistic upper bound of safety index as $\mathbf{U}_f(x, u) := \phi(\mu_f(x, u)) + L_\phi \beta_f \sigma_f(x, u)$ (Lemma 1), where we denote L_ϕ as the Lipschitz constant of $\phi(\cdot)$ with respect to 1-norm. Note that the true value of safety index $\phi(f(x, u))$ is smaller than $\mathbf{U}_f(x, u)$ with probability at least $(1 - \delta)$. The proof of this probabilistic upper bound is given in Appendix A.1.

Nonempty Set of Safe Control Since there is no white-box or black-box dynamics model, it is intractable to directly verify condition (5). On the other hand, given the probabilistic upper bound of safety index, (5) can be verified through a stricter condition, i.e. $\forall x, \exists u, \phi(f(x, u)) \leq \mathbf{U}_f(x, u) < \max\{\phi(x) - \eta, 0\}$. However, verifying this condition on the continuous state space is still intractable. Therefore, we consider a discretization of the state space defined as follows.

Definition 2 (Discretization). A τ -discretization \mathcal{H}_τ of a set \mathcal{H} is defined as $\mathcal{H}_\tau := \{h_1, h_2, \dots\}$ such that $\forall h \in \mathcal{H}, \exists h_i \in \mathcal{H}_\tau$ s.t. $\|h_i - h\|_1 \leq \tau$.

Definition 3 (Data). A dataset on a state space τ -discretization \mathcal{X}_τ is a collection of transition samples defined as $\mathcal{D}_\tau := \{(x_i, u_i, f(x_i, u_i))\}_{i=1}^{|\mathcal{X}_\tau|}$ where $x_i \in \mathcal{X}_\tau$.

Given this discretization, if we ensure the existence of safe control for states in \mathcal{X}_τ , together with the Lipschitz continuity and the bound on posterior variance of statistical models, then we can ensure the existence of safe control on the continuous state space \mathcal{X} .

Proposition 1 (Equivalence in Feasibility Conditions). With the GP defined in Definition 1, the state-space τ_x -discretization \mathcal{X}_{τ_x} defined in Definition 2 and the dataset \mathcal{D}_{τ_x} defined in Definition 3, under Assumption 1 and 2, if the following condition holds:

$$\begin{aligned} \forall (x_i, u_i), \mathbf{U}_f(x_i, u_i) &< \max\{\phi(x_i) - \eta, 0\} - L_\phi L_f \tau_x \\ &- L_\phi \tau_x - 2L_\phi \beta_f \tilde{\sigma}_f, \end{aligned} \quad (6)$$

where

$$\tilde{\sigma}_f = n_x \sqrt{2L_k \tau_x + 2|\mathcal{X}_{\tau_x}| L_k \tau_x \|K^{-1}\| \max_{w, w' \in \mathcal{W}} k(w, w')},$$

then it holds with probability $1 - \delta$ that

$$\forall x \in \mathcal{X}, \exists u \in \mathcal{U}, \text{ s.t. } \mathbf{U}_f(x, u) < \max(\phi(x) - \eta, 0). \quad (7)$$

The proof of Proposition 1 is given in Appendix A.6. Proposition 1 states that, in order to provide guarantee on the nonempty set of safe control in the whole continuous state space \mathcal{X} , it is sufficient to check a stricter condition (i.e., (6)) of nonempty set of safe control on the discretized state set \mathcal{X}_{τ_x} . Note that the additional bounds on discretized states \mathcal{X}_{τ_x} (i.e. $L_\phi L_f \tau_x, L_\phi \tau_x, 2L_\phi \beta_f \tilde{\sigma}_f$) of (6) become zero as the discretization constant τ goes to zero.

Synthesize Safe Index So far, we have shown that (6) implies (5). Therefore, a theory that quantifies how to parameterize safety index ϕ to make (6) hold is needed. To begin with, we first need to ensure there exists such a safety index to make (6) hold. Hence, an additional assumption is made:

Assumption 3 (Safe Control). The state space is bounded, and the infimum of the supremum of $\Delta \dot{d}$ can achieve positive, i.e., $\inf_x \sup_u \Delta \dot{d}(x, u) > 0$.

The necessity of Assumption 3 is summarized in Appendix A.2. Essentially, Assumption 3 enables a degree two system to dissipate energy (i.e., $\dot{\phi} < 0$) at all states. Under the above assumption, the safety index design rule is summarized in the following theorem:

Theorem 1 (Feasibility of Safety Index Design). Denote $d(\cdot)$ and $\dot{d}(\cdot)$ as the mappings from x to d and \dot{d} with Lipschitz constant L_{d_x} and $L_{\dot{d}_x}$ with respect to 1-norm. Under Assumption 1 to 3, if we select a state-space τ_x -discretization \mathcal{X}_{τ_x} with step size such that

$$\tau_x \leq \min \left\{ 1, \left[\frac{\inf_x \sup_u \Delta \dot{d}(x, u)}{2(L_{d_x} + L_{\dot{d}_x})(1 + L_f + 2\beta_f n_x \sqrt{2L_k} \sqrt{1 + |\mathcal{X}_{\tau_x}| \|K^{-1}\| \max_{w, w' \in \mathcal{W}} k(w, w')})} \right]^2 \right\} \quad (8)$$

and construct the corresponding dataset $\{(x_i, u_{GP,i}, f(x_i, u_{GP,i}))\}_{i=1}^{|\mathcal{X}_{\tau_x}|}$ on \mathcal{X}_{τ_x} by selecting $u_{GP,i}$ such that for any $x_i \in \mathcal{X}_{\tau_x}$

$$\underbrace{\dot{d}(f(x_i, u_{GP,i}))}_{d_{GP,i}} - \underbrace{\dot{d}(x_i)}_{d_i} > \frac{\inf_x \sup_u \Delta \dot{d}(x, u)}{2}, \quad (9)$$

and then choose the safety index parameters such that

$$\begin{cases} \sigma = 0, \\ n = 1, \\ k > \max_{x_i \in \mathcal{X}_{\tau_x}} \{ \max \{1, \Upsilon_i\} \} \end{cases} \quad (10)$$

where we denote $d_{GP,i} = d(f(x_i, u_{GP,i}))$, $d_i = d(x_i)$, and

$$\begin{aligned} \Upsilon_i &= \frac{\eta + d_i - d_{GP,i}}{\dot{d}_{GP,i} - \dot{d}_i - (L_{d_x} + L_{\dot{d}_x})(\tau_x - L_f \tau_x - 2\beta_f n_x \tilde{\sigma}_f)} \\ \tilde{\sigma}_f &= n_x \sqrt{2L_k \tau_x + 2|\mathcal{X}_{\tau_x}| L_k \tau_x \|K^{-1}\| \max_{w, w' \in \mathcal{W}} k(w, w')}, \end{aligned}$$

then the existence of safe control for all discretized states is guaranteed:

$$\begin{aligned} \forall x_i \in \mathcal{X}_\tau, \exists u \in \mathcal{U}, \text{ s.t.} \\ \mathbf{U}_f(f(x_i, u)) &< \max\{\phi(x_i) - \eta, 0\} - L_\phi L_f \tau_x \\ &- L_\phi \tau_x - 2L_\phi \beta_f \tilde{\sigma}_f. \end{aligned} \quad (11)$$

The proof for Theorem 1 is summarized in Appendix A.9. Theorem 1 states that, firstly, we select a proper discretization gap of state space such that it is small enough according to (8). Secondly, we construct an offline dataset such that the selected control for each discretized state can increase \dot{d} by a certain volume according to (9). Lastly, by performing GP regression on the constructed dataset, the safety index designed according to (10) ensures the existence of probabilistic safe control for all discretized states to satisfy (11).

Note that (11) is essentially the stricter condition defined in (6) on discretized domain \mathcal{X}_τ for Proposition 1. This means by satisfying the conditions of Theorem 1, we can ensure the existence of safe control on the continuous state space \mathcal{X} . The following theorem is thus a direct consequence of Proposition 1 and Theorem 1.

Theorem 2. Under the same assumptions of Theorem 1, by selecting state discretization step size according to (8), constructing Gaussian process dataset according to (9), and defining safety index according to (10), then it holds with probability $1 - \sigma$ that

$$\begin{aligned} \forall x \in \mathcal{X}, \exists u, \text{ s.t.} \\ \phi(f(x, u)) \leq \mathbf{U}_f(x, u) < \max(\phi(x) - \eta, 0). \end{aligned} \quad (12)$$

4.2 Infimum of Supremum Safety Status Change

It is worth noting that the system property $\inf_x \sup_u \Delta \dot{d}(x, u)$ is crucial for establishing the nonempty set of safe control theorem as indicated in (8) and (9). In fact, if little prior knowledge of the unknown dynamics function $f(\cdot)$ is given, it is intractable to derive the specific value of $\inf_x \sup_u \Delta \dot{d}(x, u)$. However, under a mild assumption

regarding the Lipschitz continuity of $\Delta\dot{d}(x, u)$, we can derive the lower bound of $\inf_x \sup_u \Delta\dot{d}(x, u)$, which is summarized in the following proposition.

Theorem 3. *Under Assumption 3. Consider a state-space $\tilde{\tau}$ -discretization $\mathcal{X}_{\tilde{\tau}}$ defined in Definition 2.*

For each discretized state x_i , perform grid sampling by iteratively increasing sampling resolution to find a control u_{safe_i} , s.t. $\Delta\dot{d}(x_i, u_{safe_i}) > 0$.

Denote $L_{\Delta\dot{d}}$ as the Lipschitz constant for function $\Delta\dot{d}(x, u) : \mathcal{U} \rightarrow \mathbb{R}$. Then, the system property $\inf_x \sup_u \Delta\dot{d}(x, u)$ is lower bounded by:

$$\inf_x \sup_u \Delta\dot{d}(x, u) \geq \min\{\sup_{x_i} \Delta\dot{d}_1, \sup_{x_i} \Delta\dot{d}_2, \dots, \sup_{x_i} \Delta\dot{d}_{|\mathcal{X}_{\tilde{\tau}}|}\} - L_{\Delta\dot{d}}\tilde{\tau} \quad (13)$$

where $\sup_{x_i} \Delta\dot{d}_i = \Delta\dot{d}(x_i, u_{safe_i})$.

The proof for Theorem 3 is summarized in Appendix A.11, where we use (i) grid sampling and (ii) Lipschitz continuity to derive a lower bound for the maximum value of the unknown function (in our case $\Delta\dot{d}(\cdot)$).

Theorem 3 states that we first discretize the continuous state space \mathcal{X} into discretized state space $\mathcal{X}_{\tilde{\tau}}$. Then, for each discretized state x_i , we use grid sampling by iteratively increasing the sampling resolution to find a control such that safety status change is positive, which results a lower bound of $\sup_u \Delta\dot{d}(x_i, u)$ for each discretized state. In Lemma 7, we show the grid sampling procedure can be finished within finite many iterations for each discretized state.

Finally, with the Lipschitz constant of $\Delta\dot{d}(x, u)$, the lower bound of $\inf_x \sup_u \Delta\dot{d}(x, u)$ on the continuous state space \mathcal{X} can be established according to (13). Note that all the values required in (13) can be directly computed, where the Lipschitz constant $L_{\Delta\dot{d}}$ of an unknown function $\Delta\dot{d}(\cdot, \cdot)$ can be computed analytically via GP (Lederer, Umlauf, and Hirche 2019). Therefore, the lower bound of $\inf_x \sup_u \Delta\dot{d}(x, u)$ obtained with Theorem 3 can be directly used in Theorem 2 for guaranteeing nonempty set of safe control in practical applications.

5 Uncertainty-Aware Implicit Safe Set Algorithm

In the previous section, we have established solid theoretical results on the offline dataset construction and safety index design to ensure nonempty set of safe control without white-box or black-box dynamics models. Note that the GP dynamics model is not control-affine, whereas conventional QP-based projection (Cheng et al. 2019; Dalal et al. 2018) does not work. Therefore, we leverage multi-directional line search to solve the black-box optimization in (4). In this section, we provide a practical algorithm to safeguard any RL policy building on top of (i) theories from the previous section, and (ii) a sample-efficient black-box constrained optimization algorithm (Zhao, He, and Liu 2021). In particular, we introduce Uncertainty-Aware Safe Set Algorithm (UAISSA), which is summarized in Algorithm 1.

Algorithm 1: Uncertainty-Aware Implicit Safe Set Algorithm (UAISSA)

- 1: **procedure** UAISSA(π)
 - 2: **Offline Stage:**
 - 3: Compute the lower bound of $\inf_x \sup_u \Delta\dot{d}(x, u)$ according to (13)
 - 4: Select state discretization step size τ according to (8)
 - 5: Construct dynamics learning dataset on discretized states satisfying (9)
 - 6: Perform Gaussian process on the dataset and choose safety index according to (10)
 - 7: **Online Stage:**
 - 8: **for** $t = 0, 1, 2, \dots$ **do**
 - 9: Obtain reference control $u_t^r \leftarrow \pi(x_t)$
 - 10: Solve (4) to obtain safe control u_t via Implicit Safe Set Algorithm (ISSA) [Algorithm 2, (Zhao, He, and Liu 2021)], s.t. safety status of u_t is *SAFE* (i.e., $\bigcup_f(x_t, u_t) < \max(\phi(x_t) - \eta, 0)$)
 - 11: Apply u_t to the control system
-

To have a better understanding on the *Offline Stage* of UAISSA, we summarize the procedure for constructing a valid safety index and the associated GP dynamics model in Figure 1. There are two major parts for the *Offline Stage*, which are highlighted with orange and blue backgrounds.

1) Firstly, we will discretize the state space into $\mathcal{X}_{\tilde{\tau}}$ with step size $\tilde{\tau}$. For each discretized state x_i , we apply grid sampling to find a control u_{safe_i} , such that $\Delta\dot{d}(x_i, u_{safe_i}) > 0$. Hence, we can obtain the lower bound of $\inf_x \sup_u \Delta\dot{d}(x, u)$. In order to evaluate (8), the lower bound of $\inf_x \sup_u \Delta\dot{d}(x, u)$ should be positive. In the case where lower bound of $\inf_x \sup_u \Delta\dot{d}(x, u)$ is negative, we then consider a smaller $\tilde{\tau}$ -discretization.

2) Secondly, we randomly select a discretization step size τ , and perform another τ -discretization of the state space. For each discretized state x_i , we use sampling (grid sampling or random sampling) to find a control $u_{GP,i}$ satisfying (9), which results a dynamics learning dataset $\{(x_i, u_{GP,i}, f(x_i, u_{GP,i}))\}_{i=1}^{|\mathcal{X}_{\tau}|}$. Next, we learn GP dynamics model from the constructed dataset, i.e. posterior mean and variance function. Together with the lower bound of $\inf_x \sup_u \Delta\dot{d}(x, u)$ and learned GP dynamics model, we can then evaluate (8). If (8) doesn't hold, we will further shrink the discretization step size by half, and repeat the forward mentioned procedures. If (8) holds, we will evaluate Υ_i for each x_i from the dataset, and select safety index $\phi(x)$ parameterization according to (10).

With the guarantee of nonempty set of safe control provided by Theorem 2, and the fact that ISSA can always find a suboptimal solution of (4) with finite iterations if the set of safe control is non-empty [Proposition 2, (Zhao, He, and Liu 2021)], the following theorem is thus a direct consequence of Theorem 1 from (Zhao, He, and Liu 2021).

Theorem 4 (Forward Invariance). *If the control system satisfies Assumption 1 and 3 and Gaussian process of Theorem 1, then it holds with probability $1 - \sigma$ that the Uncertainty-*

Aware Implicit Safe Set Algorithm guarantees forward invariance in the set $\mathcal{X}_S \cap \mathcal{X}_S^D$.

6 Experiment

We evaluate UAISSA in two experiments: (i) Robot arm, where we investigate the effect of applying Theorem 2 and Theorem 3 to safeguard an unknown robotics manipulator system; (ii) Safety Gym, where we apply UAISSA to safeguard unknown complex systems.

6.1 Robot Arm

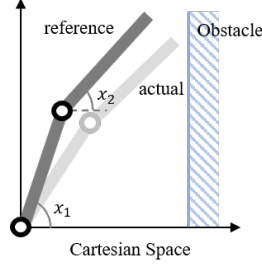


Figure 2: 2DOFs robot manipulator.

We verify our approach on a planar robotics manipulator with 2 degrees of freedom (2DOFs). The robot has a four dimensional state space: $x = [\theta_1, \theta_2, \dot{\theta}_1, \dot{\theta}_2]$, where θ_i is the i -th joint angle in the world frame. We consider limited state space, i.e., $\theta_1 \in [0, \pi]$, $\theta_2 \in [0, 2\pi]$, $\forall i = 1, 2, \dot{\theta}_i \in [-0.1, 0.1]$. The system inputs are accelerations of the two joints, i.e. $[\ddot{\theta}_1, \ddot{\theta}_2]$. The acceleration is limited such that $\forall i = 1, 2, \ddot{\theta}_i \in [-4, 4]$. The system is a discrete-time system with step size $dt = 1\text{ms}$. The system is shown in Figure 2, where the robot is randomly exploring the environment and we need to safeguard the robot from colliding with the wall.

To apply Theorems 2 and 3, we consider $L_f, L_{\Delta \dot{x}}, L_{d_x}, L_{\dot{d}_x}$ to be known. To fulfill Assumption 2, we apply a uniform error bound theory (Lemma 5 in Appendix A.7) with $\delta = 1\%$ (i.e., 99% confidence interval). The offline stage of UAISSA results (i) a discretization step of $\tau_x = 0.17$ and (ii) a safety index parameterization of: $\sigma = 0, n = 1, k = 2.54$ with $\eta = 0.05$. Then, Theorem 2 guarantees the nonempty set of safe control for (12). We simulate the system for 2000 time steps, and the evolution of $\mathbf{U}_f(x, u)$ (orange curves) and $\phi(f(x, u))$ (blue curves) is summarized in Figure 3. Overall, by ensuring $\mathbf{U}_f(x, u) < \max(\phi(x) - \eta, 0)$, UAISSA ensures $\phi(f(x, u)) < \max(\phi(x) - \eta, 0)$ along the simulations.

Furthermore, We conduct an ablation study on different discretization gap τ . The results are shown in Figure 4, where the gap between the upper bound of the safety index and the safety index decreases with smaller discretization gaps. This result echoes our theoretical results as smaller discretization gaps result in smaller error bounds of the safety index. In practice, we believe a smaller discretization gap is beneficial to the performance of robot controllers since more accurate estimates of $\mathbf{U}_f(x, u)$ alleviate the performance drop caused by conservative safeguards. However, note that smaller discretization gaps also result in large datasets which may be

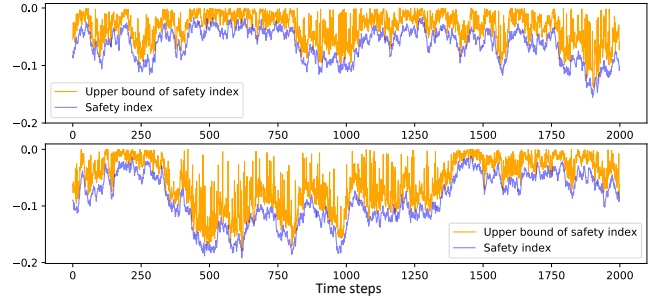


Figure 3: Evolutions of safety index and its upper bound with UAISSA over two runs.

computationally expensive for GP. It is a trade-off between lower computational cost and better performance.

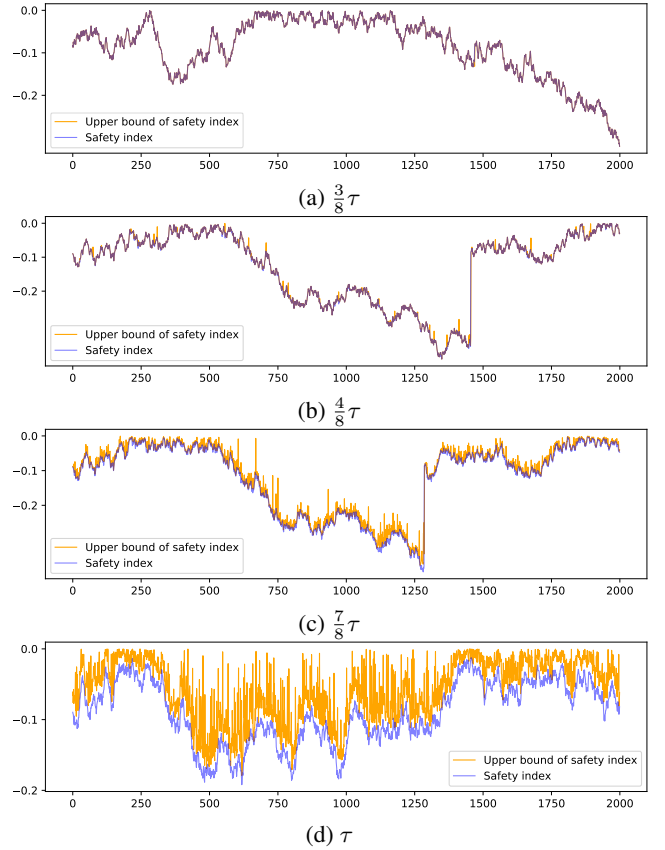


Figure 4: Evolutions of safety index and its upper bound with UAISSA with different discretization gap.

6.2 Safety Gym

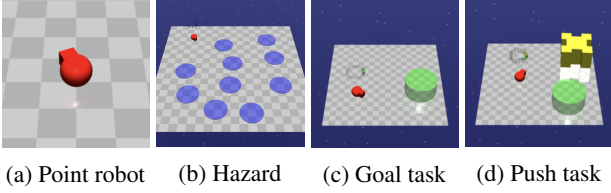


Figure 5: Robots, obstacles and tasks in Safety Gym.

Environment Setting To test how UAISSA safeguards RL policies in high-dimensional complex environments, we conduct experiments on a widely adopted benchmark of safe RL, i.e. Safety Gym (Ray, Achiam, and Amodei 2019). We evaluate UAISSA on two different control tasks (namely Goal-Hazard and Push-Hazard), where the environment settings are introduced in Figure 5. Some key elements of the environment are listed below.

- **Point Robot:** A 2D robot that can turn and move as shown in Figure 5a, with one actuator for turning and another for moving forward/backwards.
- **Hazard:** Dangerous areas to avoid as shown in Figure 5b. These are circles on the ground that are non-physical, and the robot is penalized for entering them.
- **Goal Task:** Move the robot to a series of goal positions as shown in Figure 5c.
- **Push Task:** The robot needs to push the yellow box inside the green goal area as shown in Figure 5d.

State Space The state space is composed of various physical quantities from standard robot sensors (accelerometer, gyroscope, magnetometer, and velocimeter) and lidar (where each lidar sensor perceives objects of a single kind). The state spaces of all the test suites are summarized in Table 1 (Appendix B). In safety gym, the observation contains lidar information, which is difficult to predict. Thus, we only select accelerometer, gyroscope, magnetometer and velocimeter as state for GP prediction.

Control Space For all the experiments, the control space $\mathcal{U} \subset \mathbb{R}^2$. The first dimension $u_1 \in [-10, 10]$ is the control space of moving actuator, and second dimension $u_2 \in [-10, 10]$ is the control space of turning actuator.

Baseline Selection We choose PPO (Schulman et al. 2017) as the base RL algorithm and add UAISSA as a safeguard (namely PPO-UAISSA) upon the nominal RL policy. We compare UAISSA with (i) PPO (Schulman et al. 2017) (standard RL algorithm); (ii) PPO-Lagrangian (Chow et al. 2017) and CPO (Achiam et al. 2017) (safe RL algorithms); (iii) PPO-SL (Dalal et al. 2018) (RL with safeguards).

Policy Settings Detailed parameter settings are summarized in Table 2 (Appendix B). All the policies in our experiments use the default hyper-parameter settings hand-tuned by Safety Gym (Ray, Achiam, and Amodei 2019) except the cost limit = 0 for PPO-Lagrangian and CPO.

Evaluation Results The evaluation results are shown in Figure 6, where PPO-UAISSA achieves near zero violation while gaining comparable rewards on both tasks. Note that the violations made by PPO-UAISSA are so few (nearly 1% of violations made by standard PPO), making it hard to observe in Figure 6. Such results align with our probabilistic safety guarantee given in Theorem 4. As for safe RL methods, both CPO and PPO-Lagrangian fail to achieve zero violation even with a cost limit of zero. PPO-SL proposed in (Dalal et al. 2018) also uses learned dynamics with an offline dataset, but PPO-SL failed to reduce safety violation due to (i) the assumption of linear cost functions is unrealistic in complex environments like MuJoCo (Todorov, Erez, and Tassa 2012); (ii) the lack of quantification of the error bound from neural networks. More detailed metrics for comparison and experimental results are summarized in Appendix B.4.

7 Conclusion

In this paper, we present a safe control framework with a learned dynamics model using Gaussian process. The proposed theory guarantees (i) the nonempty set of safe control for all states, and (ii) probabilistic forward invariance to the safe set. Simulation results on a robot arm and Safety Gym show near zero violation safety performance. We believe our study provides important insights into theoretical safety guarantees for policy learning.

References

- Achiam, J.; Held, D.; Tamar, A.; and Abbeel, P. 2017. Constrained policy optimization. In *International conference on machine learning*, 22–31. PMLR.
- Ames, A. D.; Grizzle, J. W.; and Tabuada, P. 2014. Control barrier function based quadratic programs with application to adaptive cruise control. In *53rd IEEE Conference on Decision and Control*, 6271–6278. IEEE.
- Beckenbach, E. 1966. On Hölder’s inequality. *Journal of Mathematical Analysis and Applications*, 15(1): 21–29.
- Berkenkamp, F.; Turchetta, M.; Schoellig, A.; and Krause, A. 2017. Safe model-based reinforcement learning with stability guarantees. *Advances in neural information processing systems*, 30.
- Caesar, H.; Bankiti, V.; Lang, A. H.; Vora, S.; Liong, V. E.; Xu, Q.; Krishnan, A.; Pan, Y.; Baldan, G.; and Beijbom, O. 2020. nuscenes: A multimodal dataset for autonomous driving. In *Proceedings of the IEEE/CVF conference on computer vision and pattern recognition*, 11621–11631.
- Cheng, R.; Orosz, G.; Murray, R. M.; and Burdick, J. W. 2019. End-to-end safe reinforcement learning through barrier functions for safety-critical continuous control tasks. In *Proceedings of the AAAI Conference on Artificial Intelligence*, volume 33, 3387–3395.
- Chow, Y.; Ghavamzadeh, M.; Janson, L.; and Pavone, M. 2017. Risk-constrained reinforcement learning with percentile risk criteria. *The Journal of Machine Learning Research*, 18(1): 6070–6120.

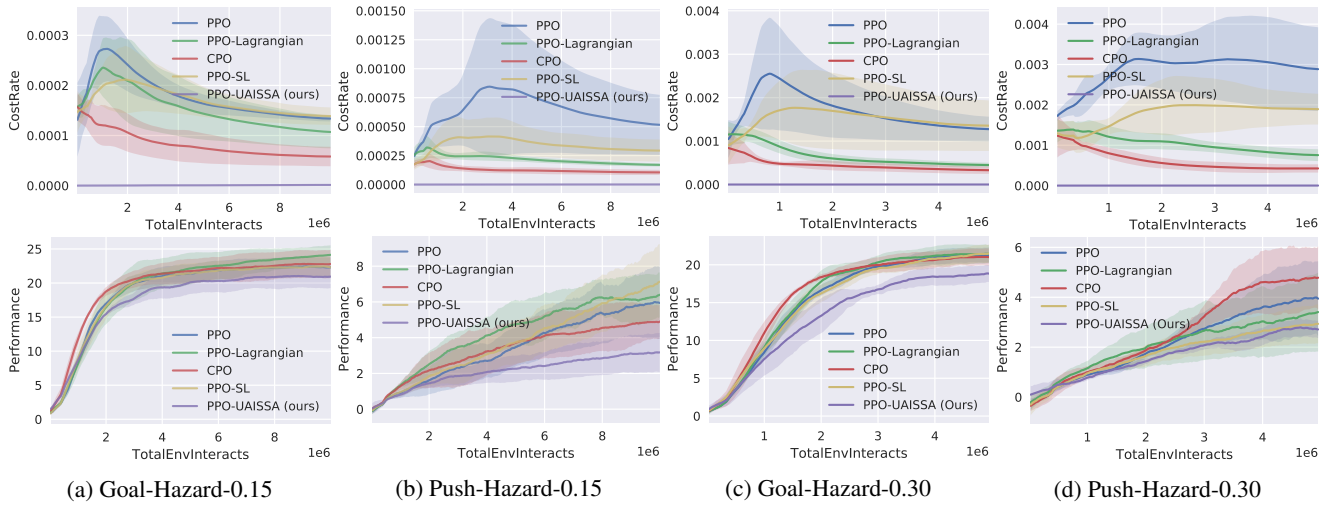


Figure 6: Cost rates and rewards of UAISSA and baselines on Safety Gym benchmarks with different tasks and sizes of the hazard over five random seeds.

Chowdhury, S. R.; and Gopalan, A. 2017. On kernelized multi-armed bandits. In *International Conference on Machine Learning*, 844–853. PMLR.

Dalal, G.; Dvijotham, K.; Vecerik, M.; Hester, T.; Paduraru, C.; and Tassa, Y. 2018. Safe exploration in continuous action spaces. *CoRR*, abs/1801.08757.

Dean, S.; Tu, S.; Matni, N.; and Recht, B. 2019. Safely learning to control the constrained linear quadratic regulator. In *2019 American Control Conference (ACC)*, 5582–5588. IEEE.

Ferlez, J.; Elnaggar, M.; Shoukry, Y.; and Fleming, C. 2020. Shieldnn: A provably safe nn filter for unsafe nn controllers. *CoRR*, abs/2006.09564.

Fisac, J. F.; Akametalu, A. K.; Zeilinger, M. N.; Kaynama, S.; Gillula, J.; and Tomlin, C. J. 2018. A general safety framework for learning-based control in uncertain robotic systems. *IEEE Transactions on Automatic Control*, 64(7): 2737–2752.

Flett, T. M. 1958. 2742. A mean value theorem. *The Mathematical Gazette*, 42(339): 38–39.

Gracia, L.; Garelli, F.; and Sala, A. 2013. Reactive sliding-mode algorithm for collision avoidance in robotic systems. *IEEE Transactions on Control Systems Technology*, 21(6): 2391–2399.

Huang, X.; Cheng, X.; Geng, Q.; Cao, B.; Zhou, D.; Wang, P.; Lin, Y.; and Yang, R. 2018. The apolloscape dataset for autonomous driving. In *Proceedings of the IEEE conference on computer vision and pattern recognition workshops*, 954–960.

Kanagawa, M.; Hennig, P.; Sejdinovic, D.; and Sriperumbudur, B. K. 2018. Gaussian processes and kernel methods: A review on connections and equivalences. *arXiv preprint arXiv:1807.02582*.

Khatib, O. 1986. Real-time obstacle avoidance for manipulators and mobile robots. In *Autonomous robot vehicles*, 396–404. Springer.

Kong, J.; Pfeiffer, M.; Schildbach, G.; and Borrelli, F. 2015. Kinematic and dynamic vehicle models for autonomous driving control design. In *2015 IEEE Intelligent Vehicles Symposium (IV)*, 1094–1099. IEEE.

Lederer, A.; Umlauft, J.; and Hirche, S. 2019. Uniform error bounds for gaussian process regression with application to safe control. *Advances in Neural Information Processing Systems*, 32.

Li, A.; Bansal, S.; Giovanis, G.; Tolani, V.; Tomlin, C.; and Chen, M. 2020. Generating robust supervision for learning-based visual navigation using hamilton-jacobi reachability. In *Learning for Dynamics and Control*, 500–510. PMLR.

Liu, C.; and Tomizuka, M. 2014. Control in a safe set: Addressing safety in human-robot interactions. In *Dynamic Systems and Control Conference*, volume 46209, V003T42A003. American Society of Mechanical Engineers.

Mnih, V.; Kavukcuoglu, K.; Silver, D.; Graves, A.; Antonoglou, I.; Wierstra, D.; and Riedmiller, M. 2013. Playing atari with deep reinforcement learning. *arXiv preprint arXiv:1312.5602*.

Ray, A.; Achiam, J.; and Amodei, D. 2019. Benchmarking safe exploration in deep reinforcement learning. *CoRR*, abs/1910.01708.

Schulman, J.; Wolski, F.; Dhariwal, P.; Radford, A.; and Klimov, O. 2017. Proximal policy optimization algorithms. *arXiv preprint arXiv:1707.06347*.

Silver, D.; Schrittwieser, J.; Simonyan, K.; Antonoglou, I.; Huang, A.; Guez, A.; Hubert, T.; Baker, L.; Lai, M.; Bolton, A.; et al. 2017. Mastering the game of go without human knowledge. *nature*, 550(7676): 354–359.

Srinivas, N.; Krause, A.; Kakade, S. M.; and Seeger, M. 2009. Gaussian process optimization in the bandit setting: No regret and experimental design. *arXiv preprint arXiv:0912.3995*.

Srinivas, N.; Krause, A.; Kakade, S. M.; and Seeger, M. W. 2012. Information-theoretic regret bounds for gaussian pro-

cess optimization in the bandit setting. IEEE transactions on information theory, 58(5): 3250–3265.

Todorov, E.; Erez, T.; and Tassa, Y. 2012. Mujoco: A physics engine for model-based control. In 2012 IEEE/RSJ International Conference on Intelligent Robots and Systems, 5026–5033. IEEE.

Uchibe, E.; and Doya, K. 2007. Constrained reinforcement learning from intrinsic and extrinsic rewards. In 2007 IEEE 6th International Conference on Development and Learning, 163–168. IEEE.

Vidyasagar, M. 2002. Nonlinear systems analysis. SIAM.

Vinyals, O.; Babuschkin, I.; Czarnecki, W. M.; Mathieu, M.; Dudzik, A.; Chung, J.; Choi, D. H.; Powell, R.; Ewalds, T.; Georgiev, P.; et al. 2019. Grandmaster level in StarCraft II using multi-agent reinforcement learning. Nature, 575(7782): 350–354.

Wachi, A.; Sui, Y.; Yue, Y.; and Ono, M. 2018. Safe exploration and optimization of constrained mdps using gaussian processes. In Proceedings of the AAAI Conference on Artificial Intelligence, volume 32.

Williams, C. K.; and Rasmussen, C. E. 2006. Gaussian processes for machine learning, volume 2. MIT press Cambridge, MA.

Yang, Q.; Simão, T. D.; Tindemans, S. H.; and Spaan, M. T. 2021. Wcsac: Worst-case soft actor critic for safety-constrained reinforcement learning. In Proceedings of the Thirty-Fifth AAAI Conference on Artificial Intelligence. AAAI Press, online.

Zhao, W.; He, T.; and Liu, C. 2021. Model-free safe control for zero-violation reinforcement learning. In 5th Annual Conference on Robot Learning.

A Theoretical Details

A.1 Error Bound of One-step Safety Index Prediction

Lemma 1. *Under Assumption 1 and Assumption 2, the one-step prediction error of the safety index is bounded with probability $1 - \delta$, i.e.,*

$$\begin{aligned} \forall x \in \mathcal{X}, \\ P(|\phi(f(x, u)) - \phi(\mu_f(x, u))| \leq |L_\phi \beta_f \sigma_f(x, u)|) \\ \geq 1 - \delta. \end{aligned} \quad (14)$$

Proof. With the Lipschitz condition, we have that with probability at least $1 - \delta$,

$$\begin{aligned} |\phi(f(x, u)) - \phi(\mu_f(x, u))| &\leq |L_\phi| |f(x, u) - \mu_f(x, u)|_1 \\ &\leq |L_\phi \beta_f \sigma_f(x, u)| \end{aligned} \quad (15)$$

□

A.2 Necessity of Assumption 3

Remark 1. *We show the necessity of Assumption 3 by contradiction. Define a subset of state space where $\mathcal{X}_d = \{x_t \in \mathcal{X} | \phi(x_t) - \eta > 0, \dot{d}_t \leq 0\}$. If the system does not satisfy Assumption 3, which means there might exists $x_t \in \mathcal{X}_d$, such that $\forall u_t \in \mathcal{U}, \Delta \dot{d}(x_t, u) \leq 0$, hence*

$$\begin{aligned} \forall u \in \mathcal{U}, \phi(x_{t+1}) - \phi(x_t) \\ = (d_{min} - d_{t+1}^n - k\dot{d}_{t+1}) - (d_{min} - d_t^n - k\dot{d}_t) \\ = (d_t^n - d_{t+1}^n) - (k\dot{d}_t - k\dot{d}_{t+1}) \\ \geq 0 - k \cdot \Delta \dot{d}(x_t, u) \\ \geq 0, \end{aligned} \quad (16)$$

which indicates the set of safe control for x_t is empty:

$$\forall u \in \mathcal{U}, \phi(x_{t+1}) \geq \max\{\phi(x_t) - \eta, 0\}. \quad (17)$$

Therefore, if the system does not satisfy Assumption 3, we cannot rule out the possibility of empty set of safe control for certain states, regardless of the safety index design. Therefore, Assumption 3 is necessary for providing guarantee on the nonempty set of safe control for all states.

A.3 Upper Bound of Posterior Variance Function

Lemma 2. *Consider a zero mean Gaussian process $g : \mathcal{Z} \rightarrow \mathbb{R}$ defined through the continuous covariance kernel $k(\cdot, \cdot)$ with Lipschitz constant L_k on the compact set \mathcal{Z} . Let $\mathcal{Z}_\tau := \{z_1, z_2, \dots, z_N\}$ be a τ -discretization set of \mathcal{Z} . Consider observations $(z_i, g(z_i))$ of g over \mathcal{Z}_τ . The posterior variance function σ_g^2 is then bounded by a constant $\tilde{\sigma}_g^2$:*

$$\begin{aligned} \forall z_* \in \mathcal{Z}, \\ \sigma_g^2(z_*) \leq \tilde{\sigma}_g^2 := 2L_k\tau + 2NL_k\tau \|K^{-1}\| \max_{z, z' \in \mathcal{Z}} k(z, z'). \end{aligned} \quad (18)$$

Proof. Since σ_g is a scalar, the difference of absolute values of the posterior variance at z_* and $z_i \in \mathcal{Z}_\tau$ can be expressed as:

$$|\sigma_g^2(z_*) - \sigma_g^2(z_i)| = |\sigma_g(z_*) + \sigma_g(z_i)| \cdot |\sigma_g(z_*) - \sigma_g(z_i)|. \quad (19)$$

Note that the standard deviation is positive semidefinite (i.e., $\sigma \geq 0$), we have

$$|\sigma_g(z_*) - \sigma_g(z_i)|^2 \leq |\sigma_g^2(z_*) - \sigma_g^2(z_i)|. \quad (20)$$

With (20), we can bound the difference of standard deviation by taking the square root of the the difference of variance. With the Cauchy-Schwarz inequality and 1-norm Lipschitz constant L_k of kernel function $k(\cdot, \cdot)$, the 1-norm difference of the variance can be bounded by

$$\begin{aligned} &\|\sigma_g^2(z_*) - \sigma_g^2(z_i)\|_1 \\ &= \|k(z_*, z_*) - k_*^T(z_*)K^{-1}k_*(z_*) \\ &\quad - k(z_i, z_i) + k_*^T(z_i)K^{-1}k_*(z_i)\|_1 \\ &\leq \|2L_k\|z_* - z_i\|_1 \leftarrow \text{Lipchitz } L_k \\ &\quad + \|k_*(z_*) - k_*(z_i)\|_2 \|K^{-1}\|_2 \|k_*(z_*) + k_*(z_i)\|_2 \\ &\quad \leftarrow \text{Cauchy-Schwarz inequality} \end{aligned} \quad (21)$$

where $\|K^{-1}\|$ denotes the Frobenius norm of the matrix K^{-1} . Note that the first term of RHS of (21) can be bounded as

$$\begin{aligned} &2L_k\|z_* - z_i\|_1 \\ &\leq 2L_k\tau. \end{aligned} \quad (22)$$

As for the second term of RHS of (21), on one hand we have

$$\begin{aligned} &\|k_*(z_*) - k_*(z_i)\|_2 \\ &\leq \sqrt{N}L_k\|z_* - z_i\|_1 \\ &\leq \sqrt{N}L_k\tau, \end{aligned} \quad (23)$$

where N is the number of data points for GP. On the other hand, we have

$$\begin{aligned} &\|k_*(z_*) + k_*(z_i)\|_2 \\ &\leq 2\sqrt{N} \max_{z, z' \in \mathcal{Z}} k(z, z'). \end{aligned} \quad (24)$$

Substituting (22), (23) and (24) into (21), we have

$$\begin{aligned} &\|\sigma_g^2(z_*) - \sigma_g^2(z_i)\|_1 \\ &\leq 2L_k\tau + \sqrt{N}L_k\tau \times \|K^{-1}\| \times 2\sqrt{N} \max_{z, z' \in \mathcal{Z}} k(z, z') \\ &\leq 2L_k\tau + 2NL_k\tau \|K^{-1}\| \max_{z, z' \in \mathcal{Z}} k(z, z'). \end{aligned} \quad (25)$$

With (20) and (25), we obtain the bound of standard deviation as

$$\begin{aligned} &\|\sigma_g(z_*) - \sigma_g(z_i)\|_1 \\ &\leq \sqrt{\|\sigma_g^2(z_*) - \sigma_g^2(z_i)\|_1} \\ &\leq \sqrt{2L_k\tau + 2NL_k\tau \|K^{-1}\| \max_{z, z' \in \mathcal{Z}} k(z, z')}. \end{aligned} \quad (26)$$

With (26), we further bound $\sigma_g(z_*)$ by the fact that $\sigma_g(z_i) = 0$ (because $(z_i, g(z_i))$ is a data point for GP) as follows.

$$\begin{aligned} & \sigma_g(z_*) \\ &= \|\sigma_g(x, u_0) - \sigma_g(z_i)\|_1 \\ &\leq \sqrt{2L_k\tau + 2NL_k\tau\|K^{-1}\| \max_{z, z' \in \mathcal{Z}} k(z, z')}. \end{aligned} \quad (27)$$

For simplicity, we denote $\tilde{\sigma}_g = \sqrt{2L_k\tau + 2NL_k\tau\|K^{-1}\| \max_{z, z' \in \mathcal{Z}} k(z, z')}$. Note that $\tilde{\sigma}_g$ is a value determined by the GP model: (i) kernel function $k(\cdot, \cdot)$ of GP; (ii) data points for GP; (iii) GP discretization gap τ . \square

A.4 Upper Bound of Posterior Mean Function

Lemma 3. Consider a zero mean Gaussian process $g : \mathcal{Z} \rightarrow \mathbb{R}$ defined through the continuous covariance kernel $k(\cdot, \cdot)$ with Lipschitz constant L_k on the compact set \mathcal{Z} . Let $\mathcal{Z}_\tau := \{z_1, z_2, \dots, z_N\}$ be a τ -discretization set of \mathcal{Z} . Consider observations $(z_i, g(z_i))$ of g over \mathcal{Z}_τ , the posterior mean function μ_g is bounded by:

$$\mu_g \leq \max\{g(z_1), g(z_2), \dots, g(z_N)\} + \sqrt{N}L_k\tau\|K^{-1}y_N\|_2. \quad (28)$$

$$\mu_g \leq \max\{g(z_1), g(z_2), \dots, g(z_N)\} + \sqrt{N}L_k\tau\|K^{-1}y_N\|_2. \quad (29)$$

Proof. According to (2), we have the posterior mean function that satisfies:

$$\mu_g(z_*) = k_*^T(z_*)K^{-1}y_N, \quad (30)$$

where $K_{i,j} = k(z_i, z_j)$ and $k_*(z_*) = [k(z_1, z_*), k(z_2, z_*), \dots, k(z_N, z_*)]^T$. With the Cauchy-Schwarz inequality and 1-norm Lipschitz constant L_k of kernel function $k(\cdot, \cdot)$, the difference of absolute values of mean function can be bounded by:

$$\begin{aligned} \|\mu_g(z_*) - \mu_g(z_i)\|_1 &= \|(k_*^T(z_*) - k_*^T(z_i))K^{-1}y_N\|_1 \\ &\leq \|k_*^T(z_*) - k_*^T(z_i)\|_2\|K^{-1}y_N\|_2 \\ &\leq \sqrt{N}L_k\|z_* - z_i\|_1\|K^{-1}y_N\|_2 \\ &\leq \sqrt{N}L_k\tau\|K^{-1}y_N\|_2 \end{aligned} \quad (31)$$

Therefore, the posterior mean function μ_g is bounded by:

$$\mu_g \leq \max\{g(z_1), g(z_2), \dots, g(z_N)\} + \sqrt{N}L_k\tau\|K^{-1}y_N\|_2. \quad (32)$$

\square

A.5 Upper Bound of Posterior Variance of Multi-Dimensional Function

Lemma 4. Consider a zero mean Gaussian process $g : \mathcal{Z} \rightarrow \mathbb{R}^D$ defined through the continuous covariance kernel $k(\cdot, \cdot)$

with Lipschitz constant L_k on the compact set \mathcal{Z} . Let $\mathcal{Z}_\tau := \{z_1, z_2, \dots, z_N\}$ be a τ -discretization set of \mathcal{Z} . Consider observations $(z_i, g(z_i))$ of g over \mathcal{Z}_τ , the posterior standard deviation function σ_g is bounded by $\tilde{\sigma}_g$:

$$\begin{aligned} & \forall z_* \in \mathcal{Z}, \\ & \sigma_g(z_*) \leq \tilde{\sigma}_g \\ &= D(2L_k\tau + 2NL_k\tau\|K^{-1}\| \max_{z, z' \in \mathcal{Z}} k(z, z'))^{\frac{1}{2}}. \end{aligned} \quad (33)$$

Remark 2. In the case of multiple output dimensions ($D > 1$), we consider GP regression on a function with one-dimensional output $g'(z, i) : \mathcal{Z} \times \mathcal{I} \rightarrow \mathbb{R}$, with the output dimension indexed by $i \in \mathcal{I} = \{1, 2, \dots, D\}$. This allows us to use the standard GP methods to provide uniform error bounds with multi-dimensional outputs (Berkenkamp et al. 2017). Then, we define the posterior distribution of Gaussian process as $\mu_g(z) = [\mu_{g'}(z, 1), \dots, \mu_{g'}(z, D)]^T$ and $\sigma_g(z) = \sum_{1 \leq i \leq D} \sigma_{g'}(z, i)$.

Proof. According to the remark, to bound $\sigma_g(z)$, we need to bound $\sigma_{g'}(z, j)$ of each dimension. As more data samples for GP could only decrease the posterior variance (Williams and Rasmussen 2006), we can bound $\sigma_{g'}(z, j)$ with less data to obtain an upper bound.

As for bounding $\sigma_{g'}(z, j)$ with less data, it means that we compute the bound for $\sigma_{g'}(z, j)$ solely with the data samples for j -th output dimension, i.e. $\mathcal{Z} \times j \rightarrow \mathbb{R}$, where $j \in \mathcal{I}$.

The proof of the bound for $\sigma_{g'}(z, j)$ is almost identical to the proof in Lemma 2, except that we replace (i) z_* with (z_*, j) , and (ii) z_i with (z_i, j) . Then, we replace $\|z_* - z_i\|_1 \leq \tau$ in (22) and (23) with

$$\|(z_*, j) - (z_i, j)\|_1 = \|z_* - z_i\|_1 + \|j - j\|_1 \leq \tau. \quad (35)$$

For most of the common kernels, e.g. RBF kernel, $k_{z, z' \in \mathcal{Z}}((z, j), (z', j)) = k_{z, z' \in \mathcal{Z}}((z), (z'))$, hence, $\sigma_{g'}(z, j)$ can be bounded as:

$$\sigma_{g'}(z_*, j) \leq (2L_k\tau + 2NL_k\tau\|K^{-1}\| \max_{z, z' \in \mathcal{Z}} k(z, z'))^{\frac{1}{2}}. \quad (36)$$

where $K_{i,j} = k(z_i, z_j)$. We can further bound σ_g based on the definition where $\sigma_g(z_*) = \sum_{j \leq D} \sigma_{g'}(z_*, j)$:

$$\begin{aligned} & \forall z_* \in \mathcal{Z}, \\ & \sigma_g(z_*) \leq \tilde{\sigma}_g \\ &= D(2L_k\tau + 2NL_k\tau\|K^{-1}\| \max_{z, z' \in \mathcal{Z}} k(z, z'))^{\frac{1}{2}}. \end{aligned} \quad (37)$$

which directly yields the result. \square

A.6 Proof of Proposition 1

Proof. Denote $A = L_\phi L_f \tau_x$, $B = L_\phi \tau_x$, and $C = 2L_\phi \beta_f \tilde{\sigma}_f$, where $\tilde{\sigma}_f = \frac{1}{n_x \sqrt{2L_k\tau_x + 2|\mathcal{X}_{\tau_x}|L_k\tau_x\|K^{-1}\| \max_{w, w' \in \mathcal{W}} k(w, w')}} =$

For any $x \in \mathcal{X}$, we denote $x_{\tau_0} = \arg \min_{x_i \in \mathcal{X}_{\tau_x}} \|x_i - x\|_1$ as the closest discretized state. We further denote (x_{τ_0}, u_0) as a data sample from \mathcal{D}_τ . Note that $\forall (x_i, u_i), \mathbf{U}_f(x_i, u_i) < \max\{\phi(x_i) - \eta, 0\} - A - B - C$.

Next, We will prove Proposition 1 by showing $\forall x \in \mathcal{X}, \mathbf{U}(x, u_0) < \max\{\phi(x) - \eta, 0\}$. We first expand the terms of $\mathbf{U}_f(x, u_0)$:

$$\begin{aligned} \mathbf{U}(x, u_0) &= \phi(\mu_f(x, u_0)) + L_\phi \beta_f \sigma_f(x, u_0) \\ &= \phi(\mu_f(x, u_0)) - \phi(f(x, u_0)) \\ &\quad + \phi(f(x, u_0)) + L_\phi \beta_f \sigma_f(x, u_0) \end{aligned} \quad (39)$$

Based on Lipschitz condition in Assumption 1 and error bound in Assumption 2, the following inequality derived from (39) holds with probability at least $1 - \delta$:

$$\begin{aligned} \mathbf{U}(x, u_0) &\leq L_\phi \|\mu_f(x, u_0) - f(x, u_0)\|_1 \\ &\quad + \phi(f(x, u_0)) + L_\phi \beta_f \sigma_f(x, u_0) \\ &\quad \leftarrow \text{Lipchitz } L_\phi \\ &\leq L_\phi \beta_f \sigma_f(x, u_0) + \phi(f(x, u_0)) \\ &\quad + L_\phi \beta_f \sigma_f(x, u_0) \\ &\quad \leftarrow \text{GP error bound} \\ &= \phi(f(x, u_0)) + 2L_\phi \beta_f \sigma_f(x, u_0) \\ &= \phi(f(x, u_0)) - \phi(f(x_{\tau_0}, u_0)) + \phi(f(x_{\tau_0}, u_0)) \\ &\quad + 2L_\phi \beta_f \sigma_f(x, u_0) \\ &\leq L_\phi \|f(x, u_0) - f(x_{\tau_0}, u_0)\|_1 + \mathbf{U}_f(x_{\tau_0}, u_0) \\ &\quad + 2L_\phi \beta_f \sigma_f(x, u_0) \leftarrow \text{Lipchitz } L_f \\ &\leq L_\phi L_f \|(x, u_0) - (x_{\tau_0}, u_0)\|_1 \\ &\quad + \max\{\phi(x_{\tau_0}) - \eta, 0\} - A - B - C \\ &\quad + 2L_\phi \beta_f \sigma_f(x, u_0) \end{aligned} \quad (40)$$

By definition of the discretization, we have on each grid cell that

$$\|(x, u_0) - (x_{\tau_0}, u_0)\|_1 = \|x - x_{\tau_0}\|_1 + \|u_0 - u_0\|_1 \leq \tau_x. \quad (41)$$

According to the Lipschitz property of safety index ϕ , we also have the following condition holds:

$$\|\phi(x) - \phi(x_{\tau_0})\|_1 \leq L_\phi \|x - x_{\tau_0}\|_1 = L_\phi \tau_x \quad (42)$$

which indicates that $\phi(x_{\tau_0}) \leq \phi(x) + L_\phi \tau_x$, hence:

$$\max\{\phi(x_{\tau_0}) - \eta, 0\} \leq \max\{\phi(x) - \eta + L_\phi \tau_x, L_\phi \tau_x\}. \quad (43)$$

To bound $\sigma_f(x, u_0)$ in (40), we can follow a similar proof in Lemma 4 by replacing (i) z_* with (x, u_0) , and (ii) z_i with

(x_{τ_0}, u_0) . Therefore, we can replace $\|z_* - z_i\| \leq \tau$ in (35) with

$$\|(x, u_0) - (x_{\tau_0}, u_0)\|_1 = \|x - x_{\tau_0}\|_1 + \|u_0 - u_0\|_1 \leq \tau_x. \quad (44)$$

Since (x_{τ_0}, u_0) is a data sample from \mathcal{D}_τ , then $\sigma_f(x_{\tau_0}, u_0) = 0$, a similar inequality as (37) can be established, indicating

$$\begin{aligned} \sigma_f(x, u_0) &\leq \tilde{\sigma}_f \\ &= n_x \sqrt{2L_k \tau_x + 2|\mathcal{X}_{\tau_x}| L_k \tau_x \|K^{-1}\| \max_{w, w' \in \mathcal{W}} k(w, w')}. \end{aligned} \quad (45)$$

Plugging (41), (43) and (45) into (40), we have that

$$\begin{aligned} \mathbf{U}_f(x, u) &\leq L_\phi L_f \tau_x + \max\{\phi(x_{\tau_0}) - \eta, 0\} - A - B - C \\ &\quad + 2L_\phi \beta_f \sigma_f(x, u) \\ &\leq (L_\phi L_f \tau_x - A) + (\max\{\phi(x_{\tau_0}) - \eta, 0\} - B) \\ &\quad + (2L_\phi \beta_f \sigma_f(x, u) - C) \\ &= (L_\phi L_f \tau_x - L_\phi L_f \tau_x) + (\max\{\phi(x_{\tau_0}) - \eta, 0\} - L_\phi \tau_x) \\ &\quad + (2L_\phi \beta_f \sigma_f(x, u) - 2L_\phi \beta_f \tilde{\sigma}_f(x, u)) \\ &= 0 + (\max\{\phi(x) - \eta + L_\phi \tau_x, L_\phi \tau_x\} - B) + 0 \\ &= \max\{\phi(x) - \eta, 0\}, \end{aligned} \quad (46)$$

which directly yields the result. \square

A.7 Probabilistic Uniform Error Bound Leveraging Lipschitz Continuity of Unknown Function

In this subsection, we can construct high-probability confidence intervals on the unknown system dynamics in (1) that fulfill Assumption 2 using the Gaussian process model leveraging the Lipschitz continuity of unknown function.

Lemma 5 (Lederer, Umlauft, and Hirche 2019), Theorem 3.3). Assume a zero mean Gaussian process defined through the continuous covariance kernel $k(\cdot, \cdot)$ with Lipschitz constant L_k on the set \mathcal{Z} . Furthermore, assume a continuous unknown function $g : \mathcal{Z} \rightarrow \mathbb{R}$ with Lipschitz constant L_g and $N \in \mathbb{N}$ observations y_i . Then, the posterior mean function $\mu_g(\cdot)$ and standard deviation $\sigma_g(\cdot)$ of a Gaussian process conditioned on the training data $\{(z_i, y(z_i))\}_{i=1}^N$ are continuous with Lipschitz constant L_{μ_g} and modulus of continuity $\omega_{\sigma_N}(\cdot)$ on \mathcal{Z} such that

$$L_{\mu_g} \leq L_k \sqrt{N} \|(K + \sigma_{\text{noise}}^2 I_N)^{-1} y_N\| \quad (47)$$

$$\omega_{\sigma_N}(\tau) \leq \sqrt{2\tau L_k (1 + N \|K + \sigma_{\text{noise}}^2 I_N\|)^{-1} \max_{z, z' \in \mathcal{Z}} k(z, z')}. \quad (48)$$

$$\leq \sqrt{2\tau L_k (1 + N \|K + \sigma_{\text{noise}}^2 I_N\|)^{-1} \max_{z, z' \in \mathcal{Z}} k(z, z')}. \quad (49)$$

Moreover, pick $\delta \in (0, 1)$, $\tau \in \mathbb{R}_+$ and set

$$\beta(\tau) = 2 \log \left(\frac{M(\tau, \mathbb{Z})}{\sigma} \right) \quad (49)$$

$$\gamma(\tau) = (L_{\mu_N} + L_g) \tau + \sqrt{\beta(\tau)} \omega_{\sigma_N}(\tau). \quad (50)$$

Then, it holds that

$$P(|g(z) - \mu_g(z)| \leq \sqrt{\beta(\tau)}\sigma_g(z) + \gamma(\tau), \forall z \in \mathcal{Z}) \geq 1 - \delta. \quad (51)$$

Note that τ can be chosen arbitrarily small such that the effect of the constant $\gamma(\tau)$ can always be reduced to an amount which is negligible compared to $\sqrt{\beta(\tau)}\sigma_N(x)$.

A.8 Lipschitz Constant for Safety Index

Lemma 6. Denote the safety index design parameterization $\{n, k\}$, and denote L_{d_x} and $L_{\dot{d}_x}$ as the 1-norm Lipschitz constant of d and \dot{d} with respect to x . The 1-norm Lipschitz constant for safety index is $L_\phi = \max\{nd_{min}^{n-1}, k\}(L_{d_x} + L_{\dot{d}_x})$ when $0 < n < 1$, and $L_\phi = \max\{nd_{max}^{n-1}, k\}(L_{d_x} + L_{\dot{d}_x})$ when $n \geq 1$.

Proof. To derive the 1-norm Lipschitz constant L_ϕ of ϕ with respect to x , we first derive the 1-norm Lipschitz constant $L_{\phi_{d,\dot{d}}}$ of ϕ with respect to $\{d, \dot{d}\}$. Since the safety index $\phi(d, \dot{d}) = \sigma + d_{min}^n - d^n - kd\dot{d}$ is a continuous and differentiable function on a convex state space, where $d \in [d_{min}, d_{max}]$ and $\dot{d} \in [\dot{d}_{min}, \dot{d}_{max}]$. For any $x, y \in \mathcal{D}$, we define $\Phi(c) = \phi((1-c)x + cy)$. Since $\Phi(c)$ is a continuous function with respect to c , we have

$$\Phi(1) - \Phi(0) = \nabla_c \Phi(c)(1-0) \quad (52)$$

for some $c \in [0, 1]$ according to the mean value theorem (Flett 1958).

Since $\Phi(1) = \phi(y)$, and $\Phi(0) = \phi(x)$, the following equation holds

$$\begin{aligned} \phi(y) - \phi(x) &= \nabla_c \Phi(c) \\ &= \frac{\partial \phi((1-c)x + cy)}{\partial((1-c)x + cy)} \frac{\partial((1-c)x + cy)}{\partial c} \\ &= \nabla \phi(z)(y-x) \end{aligned} \quad (53)$$

for some $z = (1-c)x + cy$ within the line segment between x and y . According to Hölder's inequality (Beckenbach 1966), the following condition holds:

$$\begin{aligned} \|\phi(y) - \phi(x)\|_1 &\leq \|\nabla \phi(z)\|_\infty \|y - x\|_1 \\ \frac{\|\phi(y) - \phi(x)\|_1}{\|y - x\|_1} &\leq \|\nabla \phi(z)\|_\infty \end{aligned} \quad (54)$$

Since $\nabla \phi = [-nd^{n-1}, -k]^T$, we have

$$\max \|\nabla \phi\|_\infty = \left\| \begin{bmatrix} \max_d nd^{n-1} \\ k \end{bmatrix} \right\|_\infty \quad (55)$$

Note that $\max_d nd^{n-1} = nd_{min}^{n-1}$ when $0 < n < 1$, and $\max_d nd^{n-1} = nd_{max}^{n-1}$ when $n \geq 1$. Therefore, by setting $L_{\phi_{d,\dot{d}}} = \|[nd_{min}^{n-1}, k]^T\|_\infty = \max\{nd_{min}^{n-1}, k\}$ when $0 < n < 1$, and $L_{\phi_{d,\dot{d}}} = \|[nd_{max}^{n-1}, k]^T\|_\infty = \max\{nd_{max}^{n-1}, k\}$ when $n \geq 1$, the following condition holds:

$$L_{\phi_{d,\dot{d}}} = \max \|\nabla \phi\|_\infty \geq \|\nabla \phi(z)\|_\infty \geq \frac{\|\phi(y) - \phi(x)\|_1}{\|y - x\|_1}. \quad (56)$$

With the 1-norm Lipschitz constant $L_{\phi_{d,\dot{d}}}$ of ϕ with respect to $\{d, \dot{d}\}$, we can derive the 1-norm Lipschitz constant L_ϕ of ϕ with respect to x :

$$\begin{aligned} &|\phi(x_1) - \phi(x_2)| \\ &= |\phi(d(x_1), \dot{d}(x_1)) - \phi(d(x_2), \dot{d}(x_2))| \\ &\leq L_{\phi_{d,\dot{d}}} |(d(x_1), \dot{d}(x_1)) - (d(x_2), \dot{d}(x_2))| \\ &= L_{\phi_{d,\dot{d}}} (|d(x_1) - d(x_2)| + |\dot{d}(x_1) - \dot{d}(x_2)|) \\ &\leq L_{\phi_{d,\dot{d}}} L_{d_x} |x_1 - x_2| + L_{\phi_{d,\dot{d}}} L_{\dot{d}_x} |x_1 - x_2| \\ &\leq L_{\phi_{d,\dot{d}}} (L_{d_x} + L_{\dot{d}_x}) |x_1 - x_2|, \end{aligned} \quad (57)$$

where denote L_{d_x} and $L_{\dot{d}_x}$ as the 1-norm Lipschitz constant of d and \dot{d} with respect to x . As shown in (57), the last inequality is essentially the definition of the 1-norm Lipschitz constant L_ϕ of ϕ with respect to x . Therefore we have:

$$L_\phi = L_{\phi_{d,\dot{d}}} (L_{d_x} + L_{\dot{d}_x}). \quad (58)$$

□

A.9 Proof of Theorem 1

Proof. Since $\mathbf{U}_f(f(x_\tau, u)) = \phi(\mu_f(x_\tau, u)) + L_\phi \beta_f \sigma_f(x_\tau, u)$, the fundamental condition for the nonempty set of safe control is that $\forall x_i \in \mathcal{X}_{\tau_x}$,

$$\exists u \in \mathcal{U}, \text{ s.t.} \quad (59)$$

$$\begin{aligned} &\phi_\theta(\mu_f(x_i, u)) + L_\phi \beta_f \sigma_f(x_i, u) \\ &< \max\{\phi_\theta(x_i) - \eta, 0\} - L_\phi L_f \tau_x - L_\phi \tau_x - 2L_\phi \beta_f \tilde{\sigma}_f \end{aligned}$$

where $\theta = \{\sigma, n, k\}$ is the tunable parameters of the safety index.

(59) is equivalent to (62): According to Lemma 6, and the fact that $n = 1$ according to safety index design, we have $L_\phi = \max\{1, k\}(L_{d_x} + L_{\dot{d}_x})$. Therefore, the LHS of (59) can be written as:

$$\begin{aligned} &\phi_\theta(\mu_f(x_i, u)) + L_\phi \beta_f \sigma_f(x_i, u) \\ &= \sigma + d_{min} - d(\mu_f(x_i, u)) - kd(\mu_f(x_i, u)) \\ &\quad + \max\{1, k\}(L_{d_x} + L_{\dot{d}_x}) \beta_f \sigma_f(x_i, u), \end{aligned} \quad (60)$$

where $d(\cdot)$ and $\dot{d}(\cdot)$ represent the mapping from state to d and \dot{d} respectively. Similarly, RHS of (59) can be written as:

$$\max\{\phi_\theta(x_i) - \eta, 0\} - L_\phi L_f \tau_x - L_\phi \tau_x - L_\phi L_f \tau_x \quad (61)$$

$$\begin{aligned} &- L_\phi \tau_x - 2L_\phi \beta_f \tilde{\sigma}_f(x, u) \\ &= \max\{\sigma + d_{min} - d_i - kd_i - \eta, 0\} \\ &\quad - \max\{1, k\}(L_{d_x} + L_{\dot{d}_x}) L_f \tau_x \\ &\quad - \max\{1, k\}(L_{d_x} + L_{\dot{d}_x}) \tau_x \\ &\quad - 2 \max\{1, k\}(L_{d_x} + L_{\dot{d}_x}) \beta_f \tilde{\sigma}_f(x, u), \\ &\geq \sigma + d_{min} - d_i - kd_i - \eta \\ &\quad - \max\{1, k\}(L_{d_x} + L_{\dot{d}_x}) L_f \tau_x \\ &\quad - \max\{1, k\}(L_{d_x} + L_{\dot{d}_x}) \tau_x \\ &\quad - 2 \max\{1, k\}(L_{d_x} + L_{\dot{d}_x}) \beta_f \tilde{\sigma}_f(x, u), \end{aligned}$$

where $d_i = d(x_i)$ and $\dot{d}_i = \dot{d}(x_i)$.

Since $\max\{\sigma + d_{\min} - d_i - k\dot{d}_i - \eta, 0\} \geq \sigma + d_{\min} - d_i - k\dot{d}_i - \eta$, (59) can be proved if there exists u , such that RHS of (61) is larger than RHS of (60), i.e.

$$\begin{aligned} & d(\mu_f(x_i, u)) + k\dot{d}(\mu_f(x_i, u)) \\ & - \max\{1, k\}(L_{d_x} + L_{\dot{d}_x})\beta\sigma_f(x_i, u) \\ & - d_i - k\dot{d}_i - \eta - \max\{1, k\}(L_{d_x} + L_{\dot{d}_x})L_f\tau_x \\ & - \max\{1, k\}(L_{d_x} + L_{\dot{d}_x})\tau_x \\ & - 2\max\{1, k\}(L_{d_x} + L_{\dot{d}_x})\beta_f\tilde{\sigma}_f(x, u) > 0. \end{aligned} \quad (62)$$

(62) is equivalent to (66): By choosing $u = u_{GP,i}$ from Gaussian process dataset $\{(x_i, u_{GP,i}), f(x_i, u_{GP,i})\}_{i=1}^{|\mathcal{X}_\tau|}$, we have the following three conditions hold:

$$\sigma_f(x_i, u_{GP,i}) = 0 \quad (63)$$

$$d(\mu_f(x_i, u_{GP,i})) = d_{GP,i}, \quad (64)$$

$$\dot{d}(\mu_f(x_i, u_{GP,i})) = \dot{d}_{GP,i}, \quad (65)$$

where $d_{GP,i} = d(f(x_i, u_{GP,i}))$ and $\dot{d}_{GP,i} = \dot{d}(f(x_i, u_{GP,i}))$. Therefore, by selecting $u = u_{GP,i}$ and condition (62) becomes:

$$k(\dot{d}_{GP,i} - \dot{d}_i) - (d_i - d_{GP,i}) - \eta \quad (66)$$

$$- \max\{1, k\}(L_{d_x} + L_{\dot{d}_x})L_f\tau_x$$

$$- \max\{1, k\}(L_{d_x} + L_{\dot{d}_x})\tau_x$$

$$- 2\max\{1, k\}(L_{d_x} + L_{\dot{d}_x})\beta_f n_x$$

$$\cdot \sqrt{2L_k\tau_x + 2|\mathcal{X}_\tau|L_k\tau_x\|K^{-1}\| \max_{w,w' \in \mathcal{W}} k(w, w')} > 0.$$

So far, we have shown that it is sufficient to prove (66) holds in order to show (59) holds. Next, we will show that (66) holds, given the discretization step size and safety index design.

(8) and (10) ensure (66) holds: Since the state discretization size is selected according to (8), by rearranging (8), the following condition holds:

$$\frac{\inf_x \sup_u \Delta \dot{d}(x, u)}{2} - (L_{d_x} + L_{\dot{d}_x})\sqrt{\tau_x} - \quad (67)$$

$$(L_{d_x} + L_{\dot{d}_x})L_f\sqrt{\tau_x} - \left(2\sqrt{2L_k}(L_{d_x} + L_{\dot{d}_x})\beta_f n_x$$

$$\cdot \sqrt{1 + |\mathcal{X}_\tau| \|K^{-1}\| \max_{z,z' \in \mathcal{Z}} k(z, z')}\right) \sqrt{\tau_x} > 0.$$

Since the Gaussian process dataset satisfies

$$\forall x_i, \dot{d}_{GP,i} - \dot{d}_i > \frac{\inf_x \sup_u \Delta \dot{d}(x, u)}{2}, \quad (68)$$

Hence,

$$\dot{d}_{GP,i} - \dot{d}_i - (L_{d_x} + L_{\dot{d}_x})\sqrt{\tau_x} \quad (69)$$

$$- (L_{d_x} + L_{\dot{d}_x})L_f\sqrt{\tau_x}$$

$$- \left(2\sqrt{2L_k}(L_{d_x} + L_{\dot{d}_x})\beta_f n_x$$

$$\cdot \sqrt{1 + |\mathcal{X}_\tau| \|K^{-1}\| \max_{w,w' \in \mathcal{W}} k(w, w')}\right) \sqrt{\tau_x} > 0.$$

Given the fact that $\tau_x \leq 1$ (i.e., $\tau_x < \sqrt{\tau_x}$) according to (8), (69) indicates:

$$\Omega \quad (70)$$

$$\begin{aligned} & = \dot{d}_{GP,i} - \dot{d}_i - (L_{d_x} + L_{\dot{d}_x})\tau_x - (L_{d_x} + L_{\dot{d}_x})L_f\tau_x \\ & - 2(L_{d_x} + L_{\dot{d}_x})\beta_f n_x \end{aligned}$$

$$\cdot \sqrt{2L_k\tau_x + 2|\mathcal{X}_\tau|L_k\tau_x\|K^{-1}\| \max_{w,w' \in \mathcal{W}} k(w, w')} > 0.$$

According to (10), denoting the LHS of (70) as Ω , we have

$$k > 1, \text{ and } k > \frac{\eta + d_i - d_{GP,i}}{\Omega} \quad (71)$$

With (71), the LHS of (66) becomes:

$$k\Omega - \eta - (d_i - d_{GP,i}) \quad (72)$$

$$> \frac{\eta + d_i - d_{GP,i}}{\Omega} \Omega - \eta - (d_i - d_{GP,i})$$

$$= 0,$$

which indicates (66) holds.

Hence, (66) indicates (62) holds, which further indicates (59) holds for every $x_i \in \mathcal{X}_\tau$. \square

A.10 Lower Bound of Supremum for Safety Status Change

Lemma 7 (Existence). *Under Assumption 3, then for each discretized state x_i , we can find a u_{safe_i} , s.t. $\Delta \dot{d}(x_i, u_{safe_i}) > 0$, with finite many iterations.*

Proof. Under Assumption 3, we have the infimum of the supremum of $\Delta \dot{d}$ can achieve positive, i.e., $\inf_x \sup_u \Delta \dot{d}(x, u) > 0$. Since $\Delta \dot{d}(x, u)$ is a Lipschitz continuous function, we have the existence of a non-trivial set of safe control \mathcal{U}_i^S for each discretized state x_i , such that

$$\forall u \in \mathcal{U}_i^S, \Delta \dot{d}(x_i, u) \geq 0. \quad (73)$$

Hence, the following condition holds

$$\exists \mathcal{Q} \subset \mathcal{U}_i^S, \exists \kappa > 0, \text{ s.t. } s > \kappa, \quad (74)$$

where \mathcal{Q} is a n_u -dimensional hypercube with the same length of s . Denote $\zeta_{[i]} = \max_{j,k} \|u_{[i]}^j - u_{[i]}^k\|$, where $u_{[i]}$ denotes the i -th dimension of control u , and $u^j \in \mathcal{U}_i^S, u^k \in \mathcal{U}_i^S$.

By directly applying grid sampling in \mathcal{U}_i^S with sample interval s^* at each control dimension, such that $s^* < s$. The maximum sampling time T^a for finding a control u_{safe_i} in Theorem 3 satisfies the following condition:

$$T^a < \prod_{i=1}^{n_u} \left\lceil \frac{\zeta_{[i]}}{s^*} \right\rceil, \quad (75)$$

where T^a is a finite number due to infimum condition of s in (74). Then we have proved that for each $x_i \in \mathcal{X}_\tau$, we can find a control u_{safe_i} , s.t. $\Delta \dot{d}(x_i, u_{safe_i}) > 0$, with finite many iterations with finite iteration (i.e. finite sampling time). \square

A.11 Proof for Theorem 3

Proof. With discretized state space $\mathcal{X}_{\tilde{\tau}}$, the following inequality holds:

$$\forall x \in \mathcal{X}, \sup_{u \in \mathcal{U}} \Delta \dot{d}(x, u) \geq \Delta \dot{d}(x, u^{\text{near}}) \quad (76)$$

where $u^{\text{near}} = \arg \max_{u \in \mathcal{U}} \Delta \dot{d}(x^{\text{near}}, u)$, and $x^{\text{near}} \in \mathcal{X}_{\tilde{\tau}}$ such that $\|x - x^{\text{near}}\|_1 \leq \tilde{\tau}$. According to (76), we have:

$$\begin{aligned} \forall x \in \mathcal{X}, \sup_{u \in \mathcal{U}} \Delta \dot{d}(x, u) & \geq \Delta \dot{d}(x^{\text{near}}, u^{\text{near}}) + \Delta \dot{d}(x, u^{\text{near}}) \\ & \quad - \Delta \dot{d}(x^{\text{near}}, u^{\text{near}}) \\ & \geq \Delta \dot{d}(x^{\text{near}}, u^{\text{near}}) - L_{\Delta \dot{d}} \tilde{\tau} \\ & \geq \min\{\sup \Delta \dot{d}_1, \sup \Delta \dot{d}_2, \dots, \sup \Delta \dot{d}_{|\mathcal{X}_{\tilde{\tau}}|}\} \\ & \quad - L_{\Delta \dot{d}} \tilde{\tau} \end{aligned} \quad (77)$$

where $\sup \Delta \dot{d}_i$ denotes the supremum $\Delta \dot{d}$ for i -th discretized state x_i . Therefore, the infimum of the supremum $\Delta \dot{d}$ is lower bounded by:

$$\begin{aligned} \inf_x \sup_u \Delta \dot{d}(x, u) & \geq \min\{\sup \Delta \dot{d}_1, \sup \Delta \dot{d}_2, \dots, \sup \Delta \dot{d}_{|\mathcal{X}_{\tilde{\tau}}|}\} - L_{\Delta \dot{d}} \tilde{\tau}. \end{aligned} \quad (78)$$

According to Lemma 7, for each discretized state x_i , we can find a u_{safe_i} , s.t. $\Delta \dot{d}(x_i, u_{\text{safe}_i}) > 0$. Hence, the $\sup \Delta \dot{d}_i$ is bounded by

$$\sup \Delta \dot{d}_i > \Delta \dot{d}(x_i, u_{\text{safe}_i}) = \underline{\sup \Delta \dot{d}_i}. \quad (79)$$

By plugging (79) into (78),

$$\begin{aligned} \inf_x \sup_u \Delta \dot{d}(x, u) & \geq \min\{\underline{\sup \Delta \dot{d}_1}, \underline{\sup \Delta \dot{d}_2}, \dots, \underline{\sup \Delta \dot{d}_{|\mathcal{X}_{\tilde{\tau}}|}}\} - L_{\Delta \dot{d}} \tilde{\tau}. \end{aligned} \quad (80)$$

□

B Experiment Details

B.1 Environment Settings

Goal Task In the Goal task environments, the reward function is:

$$r(x_t) = d_{t-1}^g - d_t^g + \mathbb{1}[d_t^g < R^g],$$

where d_t^g is the distance from the robot to its closest goal and R^g is the size (radius) of the goal. When a goal is achieved, the goal location is randomly reset to someplace new while keeping the rest of the layout the same.

Push Task In the Push task environments, the reward function is:

$$r(x_t) = d_{t-1}^r - d_t^r + d_{t-1}^b - d_t^b + \mathbb{1}[d_t^b < R^g],$$

where d^r and d^b are the distance from the robot to its closest goal and the distance from the box to its closest goal, and R^g is the size (radius) of the goal. The box size is 0.2 for all the Push task environments. Like the goal task, a new goal location is drawn each time a goal is achieved.

Hazard Constraint In the Hazard constraint environments, the cost function is:

$$c(x_t) = \max(0, R^h - d_t^h),$$

where d_t^h is the distance to the closest hazard and R^h is the size (radius) of the hazard. We adopt two different sizes (0.15 and 0.30) of the hazard for evaluation as shown in Figure 6.

B.2 State Space Components

The components of state space of the two environments (Goal-Hazard and Push-Hazard) in Safe Gym are shown in Table 1.

B.3 Hyper-paramters

The hyper-parameters used for evaluation in Safety Gym are reported in Table 2.

B.4 Metrics Comparison

In this section, we report all the results of eight test suites by two metrics defined in Safety Gym (Ray, Achiam, and Amodei 2019):

- The average episode return J_r .
- The average cost over the entirety of training ρ_c .

The average episode return J_r and the average episodic sum of costs M_c were obtained by averaging over the last five epochs of training to reduce noise. Cost rate ρ_c was just taken from the final epoch. We report the results of these three metrics in Table 3 normalized by PPO results.

State Space Option	Goal-Hazard	Push-Hazard
Accelerometer (\mathbb{R}^3)	✓	✓
Gyroscope (\mathbb{R}^3)	✓	✓
Magnetometer (\mathbb{R}^3)	✓	✓
Velocimeter (\mathbb{R}^3)	✓	✓
Goal Lidar (\mathbb{R}^{16})	✓	✓
Hazard Lidar (\mathbb{R}^{16})	✓	✓
Box Lidar (\mathbb{R}^{16})	✗	✓

Table 1: The state space components of different test suites environments.

Policy Parameter	PPO	PPO-Lagrangian	CPO	PPO-SL & PPO-UAISSA
Timesteps per iteration	30000	30000	30000	30000
Policy network hidden layers	(256, 256)	(256, 256)	(256, 256)	(256, 256)
Value network hidden layers	(256, 256)	(256, 256)	(256, 256)	(256, 256)
Policy learning rate	0.0004	0.0004	(N/A)	0.0004
Value learning rate	0.001	0.001	0.001	0.001
Target KL	0.01	0.01	0.01	0.01
Discounted factor γ	0.99	0.99	0.99	0.99
Advantage discounted factor λ	0.97	0.97	0.97	0.97
PPO Clipping ϵ	0.2	0.2	(N/A)	0.2
TRPO Conjugate gradient damping	(N/A)	(N/A)	0.1	(N/A)
TRPO Backtracking steps	(N/A)	(N/A)	10	(N/A)
Cost limit	(N/A)	0	0	(N/A)

Table 2: Important hyper-parameters of PPO, PPO-Lagrangian, CPO, PPO-SL and PPO-UAISSA

Algorithm	\bar{J}_r	$\bar{\rho}_c$
PPO	1.000	1.00000
PPO-Lagrangian	1.079	0.79350
CPO	1.022	0.43588
PPO-SL	0.997	1.03483
PPO-UAISSA (Ours)	0.939	0.00965

(a) Goal-Hazard1-0.05

Algorithm	\bar{J}_r	$\bar{\rho}_c$
PPO	1.000	1.00000
PPO-Lagrangian	1.107	0.32901
CPO	0.841	0.20376
PPO-SL	1.259	0.57114
PPO-UAISSA (Ours)	0.528	0.00158

(b) Push-Hazard-0.15

Algorithm	\bar{J}_r	$\bar{\rho}_c$
PPO	1.000	1.00000
PPO-Lagrangian	1.008	0.35270
CPO	0.990	0.25780
PPO-SL	1.011	1.07102
PPO-UAISSA (Ours)	0.884	0.00060

(c) Goal-Hazard-0.30

Algorithm	\bar{J}_r	$\bar{\rho}_c$
PPO	1.000	1.00000
PPO-Lagrangian	0.849	0.26067
CPO	1.192	0.14833
PPO-SL	0.757	0.66262
PPO-UAISSA (Ours)	0.689	0.00034

(d) Push-Hazard-0.30

Table 3: Normalized metrics obtained from the policies at the end of the training process, which is averaged over four test suits environments and five random seeds.